Analysis of Indirect Temperature-Rise Tests of Induction Machines Using Time Stepping Finite Element Method

S. L. Ho and W. N. Fu

***Abstract*—To be able to test the temperature-rise of induction motors with indirect loading is very useful for the motor industry. In this paper different indirect loading schemes including two-frequency methods, phantom loading methods and inverter driven methods, are surveyed. Their merits and demerits are highlighted. A universal method for analyzing all these indirect temperature-rise methods is presented. The analysis is based on the time stepping finite element model of skewed rotor bar induction machines and the solution can include the effects of saturation, eddy-current and the highorder harmonic fields directly. The computed losses can also include the stray losses due to the high-order harmonic fields. An 11 kW induction motor, when operating with normal full-load and on phantom loading, has been used to verify the computed results.**

***Index Terms*—Finite element method, induction machine, losses, temperature-rise test.**

I. Introduction

THE RESULT of full-load temperature-rise test is an important index of an electrical machine's characteristics. However, many large induction motors cannot be loaded due to:

1) The absence of a suitable load;
2) The motor cannot be coupled mechanically with the load *in situ*, especially when the motor is to be installed vertically;
3) Energy consumed during the temperature-rise test is wasted thermally in many load tests, resulting in the overheating of some equipment or devices.

Hence it will be interesting to find some indirect methods to study the temperature-rise of induction motors when facilities for direct loading is not available or when the motor cannot be loaded readily.

Some researchers have presented different methods of indirect loading schemes including two-frequency loading [1]–[5], phantom loading [6]–[9], and inverter driven methods [10], [11]. Each method requires the motor to operate at specific conditions with the possibility to generate the rated motor losses. However, because of the complicated physical process in the motor, such as the requirement of running the machine concurrently as a motor and a generator, it is difficult to carry out a thorough study using the traditionally analytical methods. As far as the authors are aware, there has not been any comprehensive investigation in assessing the thermal behavior of motors with different indirect loading methods.

Finite element method (FEM) for the computation of magnetic field provides a possibility to determine the distribution of magnetic fields in the motor. The development of FEM for electrical machines can be divided into the following stages [12]:

1) Static field of FEM;
2) Complex field of FEM;
3) Circuit-field coupled FEM;
4) Time stepping circuit-field coupled FEM.

Method 1) assumes the magnetic field is static while methods 2) and 3) assume the fields are varying sinusoidally in time. Method 4) allows the waveforms of the magnetic potentials, currents and torque in the time domain to have arbitrary shapes. Therefore, the time stepping circuitfield coupled FEM can be used to compute the transient process of the magnetic field and to evaluate the high-order harmonic stray losses as well.

In this paper the indirect temperature-rise methods are reviewed first. Their merits and demerits, as well as possible applications are discussed. A time stepping finite element method is then proposed to simulate the indirect test methods. The proposed algorithm can precisely take into account the effects of saturation, eddy-current and high-order harmonic fields in the solutions. An 11 kW induction motor operating at normal full-load and on phantom loading condition, has been used to verify the computed results.

II. Review of Indirect Temperature-Rise Methods

In all indirect temperature-rise methods no mechanical coupling to the motor shaft is necessary.

A. Two-Frequency Method

As early as 1921, Ytterberg has proposed to connect two voltage supplies of different frequencies in series to drive an induction motor [1]. The main voltage v_1 has a rated frequency f_1. The auxiliary voltage v_2 has a lower frequency f_2 (about 60–95% of f_1) and its magnitude is about 5–25% of the mains voltage. v_1, v_2, and f_2 are adjusted until the r.m.s values of the effective input voltage and stator current are equal to their respective rated values. The voltage at the terminal of the stator winding is

$$v = \sqrt{2}\,V_1\,\cos(2\pi f_1) + \sqrt{2}\,V_2\,\cos(2\pi f_2). \qquad (1)$$

Manuscript received November 19, 1999. This work was supported by the Hong Kong Polytechnic University.

The authors are with the Department of Electrical Engineering, The Hong Kong Polytechnic University, Kowloon, Hong Kong.

Publisher Item Identifier S 0885-8969(01)02656-0.

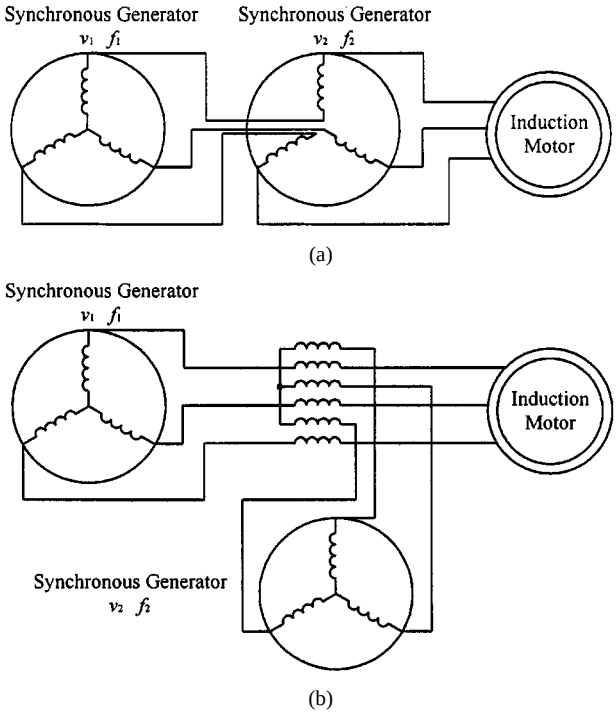

Fig. 1. Two possible schematics for performing two-frequency method.

With the machine running with no mechanical shaft coupling, the rotor will oscillate around the synchronous speeds corresponding to f_1 and f_2. In essence, the machine will operate concurrently as a motor and a generator.

The two-frequency method has been used in Europe and it has been incorporated into the Japanese Test Code for Induction Motors [2]. Two possible schematics for performing the two-frequency method are shown in Fig. 1 [4]. The method requires a motor-generator set to provide the nonstandard frequency test voltage. If the main voltage source comes directly from the mains, the currents at frequency f_2 will affect the quality of the mains. Another disadvantage is that the electromagnetic torque will oscillate at $(f_1 - f_2)$ Hz. Such oscillations may cause serious problems in vertically mounted motors [3], [4]. The relatively large power swings taking place between the supplies and the induction motor may lead to transient disturbances to result in a temporary failure in the supply [5].

B. Phantom Loading

With the phantom loading method, the phase voltage of the stator winding has both a.c. and d.c. components as follows:

$$v = \sqrt{2}\,V_1 \cos(2\pi f_1) + V_{\rm dc} \tag{2}$$

where the voltage of the d.c. component is dependent on the connection of the stator windings on phantom loading.

1) Phantom Loading with Star Connection: The earliest proposed phantom loading [6] requires the motors to be reconnected essentially in star (Fig. 2), even though most industrial-sized induction motors are connected in delta. Balanced 3-phase voltages are applied and the motor runs on no-load. A d.c. current is injected into the windings and a stationary d.c. field will appear in the motor air-gap.

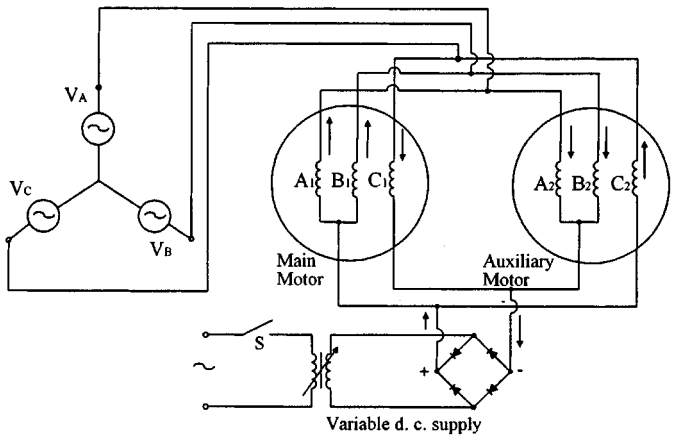

Fig. 2. Phantom loading connection for star-connected stator windings.

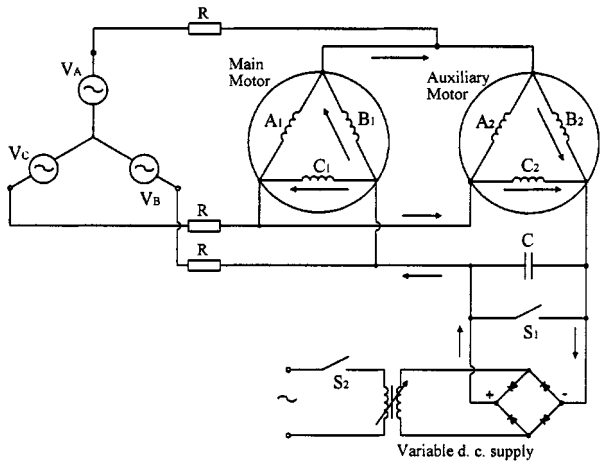

Fig. 3. Phantom loading connection for delta-connected windings.

The beauty of this star-connection is that the a.c. and d.c. sources can be feeding the two star-connected circuits at the same time independently. The disadvantage is that a voltage supply having $\sqrt{3}$ times the normal value is required if the motors are normally connected in delta. Because of the requirement for such abnormally high voltages, it is sometimes difficult to find a suitable power supply, especially for large motors, to carry out the test.

An alternative method was also presented and it was claimed that the method is more suitable for rotors with significant skin-effect [7]. Because the method requires up to 12 leads to be brought out from each of two equally rated motors, this method is not applicable to normal motors.

2) Phantom Loading with Delta Connection: One of the authors has however reported that there is another possible connection [8], [9] to inject the d.c. loading current into the windings of a delta connected motor (Fig. 3). The effective r.m.s. values of the combined a.c. and d.c. currents flowing in each of the three phase windings with such phantom loading method should be equal to the rated r.m.s. currents in the motor windings. The authors reckon that it is easier to find d.c. current/voltage injectors than finding an inverter or a voltage source which could absorb regenerated power. Phantom loading tests could then be the easiest way for indirect temperature-rise test.

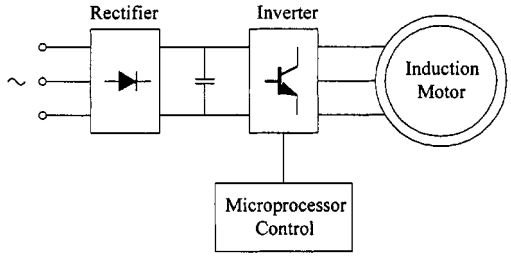

Fig. 4. Block diagram of inverter driven method.

C. Inverter Driven Method

A microprocessor can be used to generate the necessary logical control signals for a PWM inverter (Fig. 4). The microprocessor calculates the pulse widths to control the output in real time using lookup tables and some multiplication routine. Almost any output waveforms may be produced from the inverter provided that all the calculations can be completed within the time period between the narrowest output pulses.

1) Two Frequency Method by Using Inverter: The basic idea is the same as the two-frequency method but microprocessor controlled power electronics are used to generate the necessary voltages and frequencies as if two supplies are available [10].

2) Sweep Frequency Method: The input voltage to the motor is primarily a single frequency supply, but the inverter rapidly modulate the motor frequency over a small range centered at the rated frequency [10]. The input voltage is:

$$v = \sqrt{2}\,V_1 \cos\left\{\left[2\pi f_1 + \frac{\sqrt{2}\,V_2}{2\pi f_2}\,\sin(2\pi f_2 t)\right] t\right\}. \quad (3)$$

This causes alternating induction motor-generator action. Because it is not possible to produce the required change of frequency using electrical machines, this method will definitely require microprocessor controlled power electronics.

3) Magnetic Field Magnitude Modulation Method: This method uses microprocessor controlled power electronics to produce a constant speed rotating magnetic field with a sinusoidal varying amplitude in time domain [11]. The rotor speed would thus oscillate around the synchronous speed of the rotating magnetic field. Because, the rotor voltage is mainly induced by the flux wave with varying magnitude, the oscillating torque required to produce the rated currents in both the rotor and stator is expected to be small.

The inverter driven method requires a specially designed inverter and it cannot be implemented readily by the normal industrial users. It would naturally be very useful if a software can be incorporated in the inverters to produce appropriate waveforms to perform the afore-mentioned indirect load tests. The following discussion will focus on the two-frequency test and phantom load test although the analysis to be described can be extended to cover the inverter driven methods.

III. Simulation of Indirect Temperature-Rise Methods

When the input a.c. voltage waveform and the d.c. current density (only in the case of phantom loading) are known, it is necessary to find the current waveform, torque waveform and the losses distribution in all these indirect tests. A set of system equations which couples the circuit equations, FEM equations and torque equation together will constitute the numerical model which will be solved by using time stepping method. In order to deal with the skewed rotor bars, a multislice technique is used [13].

A. Circuit Equations

The stator voltage balance equation of one phase for the a.c. components is:

$$-\frac{l}{SM}\sum_{m=1}^{M}\left(\iint_{\Omega_+^{(m)}} \frac{\partial A}{\partial t}\,d\Omega - \iint_{\Omega_-^{(m)}} \frac{\partial A}{\partial t}\,d\Omega\right) + R_1 i_{\rm ac} + L_\sigma \frac{di_{\rm ac}}{dt} = v_{\rm ac} \quad (4)$$

where R_1 is the total stator resistance of one phase winding; L_σ is the inductance of the end windings. The rotor is divided axially into M slices of equal length and m stands for the mth slice; A is the axial component of the magnetic vector potential; l is the axial length of the stator iron core; S is the total cross-sectional area of one turn at one side; Ω_+ and Ω_- are, respectively, the cross-sectional areas of the "go" and "return" side of the phase conductors of the coils. $i_{\rm ac}$ and $v_{\rm ac}$ are, respectively, the a.c. components of stator current and terminal voltage.

For the two-frequency method,

$$v_{\rm ac} = \sqrt{2}\,V_1\,\cos(2\pi f_1) + \sqrt{2}\,V_2\,\cos(2\pi f_2). \quad (5)$$

For phantom loading,

$$v_{\rm ac} = \sqrt{2}\,V_1\,\cos(2\pi f_1). \quad (6)$$

In the rotor conductor domain, the circuit equations are the same as for the normal operation of induction motors [13].

B. FEM Equations

In the stator conductor domain, the field equation is:

$$\nabla \times (v\nabla \times A) - (i_{\rm ac}/S) = \pm(I_{\rm dc}/S) \quad (7)$$

where v is the reluctivity of the material. The d.c. component of the stator current $I_{\rm dc}$ is known. The sign for the current is dependent on the path of the d.c. in that particular connection. Except for phantom loading, $I_{\rm dc} = 0$. In the rotor conductor domain and in the iron domains as well as in the air-gap, the governing equations are the same as that for a normal motor [13].

C. Torque Equation

$$J_m \frac{d\omega}{dt} = T_c - T_f \quad (8)$$

where

J_m is the moment of inertia;
ω is the rotor speed;
T_f is the load torque.

The electromagnetic torque T_c is a function of A in the air-gap.

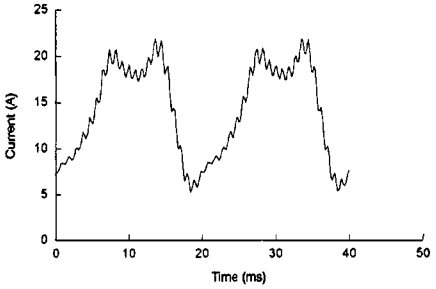

Fig. 5. Computed stator phase currents with Δ-connected stator windings carrying phantom loading.

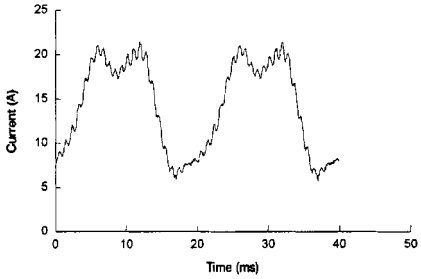

Fig. 6. Measured stator phase currents with Δ-connected stator windings carrying phantom loading.

D. Coupled System Equations

Coupling the circuit equations, the torque equation and the FEM formulation together, one obtains the large nonlinear global system of equations as follows [13]:

$$[C][A \quad i \quad \omega \quad \theta]^T + [D]\left[\frac{\partial A}{\partial t} \quad \frac{\partial i}{\partial t} \quad \frac{\partial \omega}{\partial t} \quad \frac{\partial \theta}{\partial t}\right]^T = [P] \tag{9}$$

where

the unknowns $[A]$, $[I]$, ω, and θ are, respectively, the magnetic vector potentials, the currents, the rotor speed and the position of the rotor;

$[C]$, $[D]$ are the coefficient matrices and

$[P]$ is the vector associated with the input a.c. stator phase voltages and the d.c. stator currents (in the case of phantom loading only).

The Backward Eider's method is used to discretize the time variable. The rotor FEM mesh is moved in accordance with the rotation of the rotor.

E. Computation of Losses

After the waveforms of currents, flux densities are computed, the copper loss, eddy-current loss and hysteresis loss can all be directly computed according the formulas presented by the authors. The stray losses due to the highorder harmonic have also been included [14].

IV. Results

The developed FEM modeling has been used to simulate the operation of indirect temperature-rise methods of a skewed rotor induction motor (11 kW/380 V, 50 Hz, 4 poles, 48 stator slots, 44 rotor slots, Δ connection, rotor skew of 1.3 stator slots). The time step size is 0.038 ms. The rotor is divided into 4 slices. The number of total unknowns of the FEM equations is 10 767 and the average solution time of each time stepping needs 56 s on a Pentium II/300 MHz.

A typical computed stator current waveform, the corresponding measured waveform and the computed flux distribution with the stator windings connected in delta carrying phantom loading are shown in Figs. 5–7, respectively.

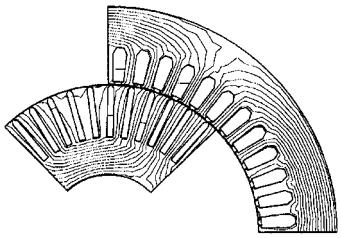

Fig. 7. Flux distribution for Δ-connected stator windings carrying phantom loading.

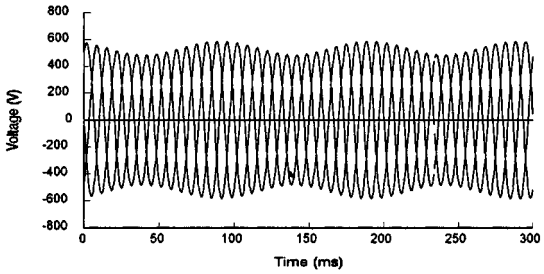

Fig. 8. Inputted three phase voltages with the two-frequency method ($f_2 = 40$ Hz, $V_2/V_1 = 9.477\%$).

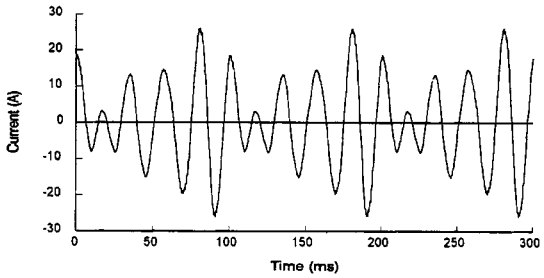

Fig. 9. Computed stator phase current with the two-frequency method ($f_2 = 40$ Hz, $V_2/V_1 = 9.477\%$).

Waveforms of the input phase voltages, computed stator current, rotor bar current, torque and speed when the motor is tested with the two-frequency supply are given in Figs. 8–12, respectively.

For the two-frequency method, the computation shows that if the r.m.s. stator current is to be kept at its rated value, V_2/V_1 should increase with increases in f_2 (Fig. 13). When the r.m.s. stator current is equal to its rated value, the computed rotor copper loss decreases with increases in f_2 (Fig. 14). The computation also indicates that the magnitude of the oscillation of the rotor speed will have a maximum value when f_2 is near 43 Hz for this case (Fig. 15).

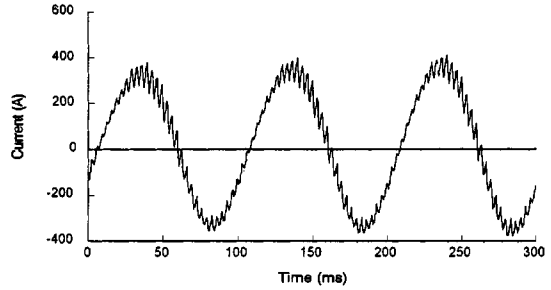

Fig. 10. Computed rotor bar current with the two-frequency method ($f_2 = 40$ Hz, $V_2/V_1 = 9.477\%$).

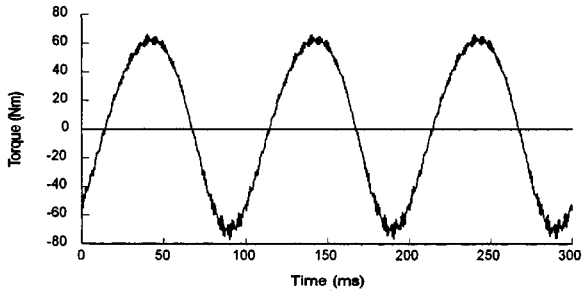

Fig. 11. Computed torque with the two-frequency method ($f_2 = 40$ Hz, $V_2/V_1 = 9.477\%$).

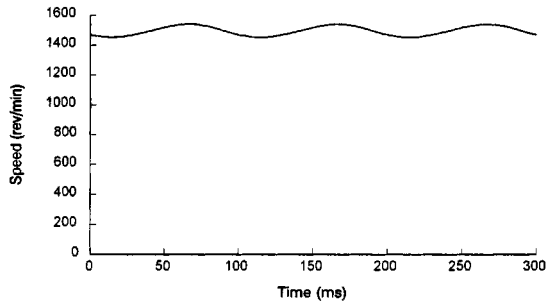

Fig. 12. Computed speed with the two-frequency method ($f_2 = 40$ Hz, $V_2/V_1 = 9.477\%$).

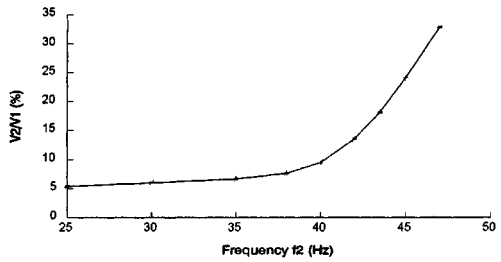

Fig. 13. Computed V_2/V_1 vs. f_2 in the two-frequency method when the r.m.s. stator current is equal to rated value.

Computed losses in the motor at rated condition, on phantom loading and the two-frequency tests are listed in Table I. The test results at rated condition and on phantom loading are given in Table II. It can be seen that there are good agreement between full load test and phantom loading.

V. Conclusion

The computed and experimental results show that phantom loading can be used to assess the temperature-rise of induction motors. The computed results of the two-frequency method reveal that when the auxiliary frequency decreases, the rotor copper loss will increase. It gives a good indication as how the auxiliary frequency should be chosen in order to give an

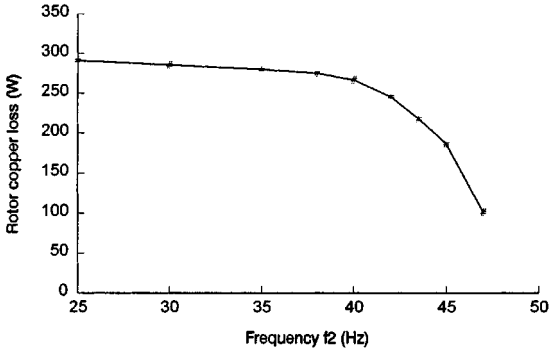

Fig. 14. Computed rotor copper loss vs. f_2 in the two-frequency method when the r.m.s. stator current is equal to rated value.

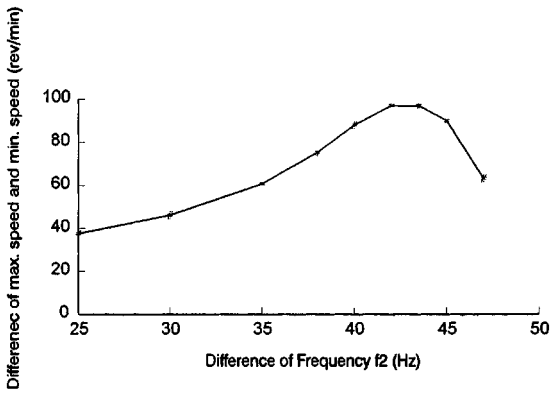

Fig. 15. Computed difference of max. speed and min. speed vs. f_2 in the two-frequency method when the r.m.s. stator current is equal to rated value.

TABLE I
COMPARISON OF COMPUTED LOSSES (W)

Method	Copper losses		Iron losses		Total
	Stator	Rotor	Stator	Rotor	
Conventional full load	584.4	263.2	163.8	85.7	1097.1
Phantom Load Y connected	586.0	241.6	170.7	138.6	1136.9
Phantom Load Δ connected	586.5	257.7	171.3	138.8	1154.3
Two-frequency (f_2=25Hz)	588.5	291.2	189.8	96.3	1165.8
Two-frequency (f_2=30Hz)	587.4	285.7	190.3	95.5	1158.9
Two-frequency (f_2=35Hz)	588.7	280.1	190.8	94.8	1154.4
Two-frequency (f_2=38Hz)	587.9	275.4	193.0	94.6	1150.9
Two-frequency (f_2=40Hz)	587.2	266.8	196.4	94.5	1144.9
Two-frequency (f_2=42Hz)	589.1	245.7	201.9	93.7	1130.4
Two-frequency (f_2=45Hz)	592.5	186.7	209.2	91.6	1080.0
Two-frequency (f_2=47Hz)	587.8	100.7	210.0	87.6	986.1

TABLE II
COMPARISON OF TEMPERATURE-RISE MEASUREMENTS BETWEEN PHANTOM LOADING AND DIRECT FULL-LOAD LOADING (K)

Method	Temperature-rise
Conventional full load	62.8
Phantom Loading Y connection	61.7
Phantom Loading Δ connection	61.9

accurate simulation of the real full-load condition on direct loading.

The proposed multi-slice 2-D time stepping FEM is an effective means to understand the physics and the order of magnitude of the various losses with indirect temperature-rise tests. The findings reported in this paper therefore provide a solid basis for those intending to use indirect temperature-rise methods to assess the thermal properties of their induction motors.

REFERENCES

[1] A. W. Kron, "Testing induction motors by means of a two frequency supply," in *ETZ-A*, vol. 94, Germany, 1973, pp. 77–82.

[2] *Standard of Japanese Electrotechnical Committee*, JEC-37-1979.

[3] H. E. Jordan, J. H. Cook, and R. L. Smith, "Synthetic load testing of induction machines," *IEEE Trans. Power Apparatus and Systems*, vol. 96, no. 4, pp. 1101–1103, July/Aug. 1977.

[4] H. R. Schwenk, "Equivalent loading of induction machines for temperature tests," *IEEE Trans. Power Apparatus and Systems*, vol. 96, no. 4, pp. 1126–1131, July/Aug. 1977.

[5] A. Meyer and H. W. Lorenzen, "Two-frequency heat run—A method of examination for three-phase induction motors," *IEEE Trans. Power Apparatus and Systems*, vol. 98, no. 6, pp. 2338–2347, Nov./Dec. 1979.

[6] W. Fong, "New temperature test for polyphase induction motors by phantom loading," *Proc. IEE*, vol. 119, no. 7, pp. 883–888, 1972.

[7] ——, "Temperature testing of skin-effect-rotor induction motors by synthetic loading," *Proc. IEE*, vol. 123, no. 6, pp. 546–548, 1976.

[8] S. L. Ho, "Further development of phantom loading in induction motors," in *International Conference on Electrical Machines*, U.K., Sept. 15–17, 1992, pp. 298–302.

[9] ——, "Study of stray losses under phantom loading conditions in induction motors," in *International Conference on Electrical Machines*, Paris, France, Sept. 5–8, 1994, pp. 548–553.

[10] G. Grantham, M. Sheng, and E. D. Spoouer, "Synthetic loading of three-phase induction motors using microprocessor controlled power electronics," *IEE Proc.–Electr. Power Appl.*, vol. 141, no. 2, pp. 101–108, Mar. 1994.

[11] M. Sheng and G. Grantham, "Synthetic loading of three-phase induction motors by magnetic field magnitude modulation," *IEE Proc.–Electr. Power Appl.*, vol. 141, no. 2, pp. 95–100, Mar. 1994.

[12] S. L. Ho and W. N. Fu, "Review and further application of finite element methods in induction motors," in *Electric Machines and Power Systems*: Taylor & Francis, 1998, vol. 26, pp. 111–125.

[13] ——, "A comprehensive approach to the solution of direct-coupled multislice model of skewed rotor induction motors using time-stepping eddy-current finite element method," *IEEE Trans. Magnetics*, vol. 33, no. 3, pp. 2265–2273, May 1997.

[14] S. L. Ho, W. N. Fu, and H. C. Wong, "Estimation of stray losses of skewed induction motors using coupled 2-D and 3-D time stepping finite element methods," *IEEE Trans. Magn.*, vol. 34, no. 5, pp. 3102–3105, Sept. 1998.

S. L. Ho was born in 1953. He obtained the B.Sc. and Ph.D. degrees in electrical engineering from the University of Warwick, U.K., in 1976 and 1979, respectively. He is currently a member of both the Institution of Electrical Engineers of the U.K. and the Hong Kong Institution of Engineers. He is at present an Associate Professor in the Department of Electrical Engineering, the Hong Kong Polytechnic University, Kowloon, Hong Kong. He is the holder of several patents and he has published over 100 papers in leading journals and in international conferences. His main research interests include the application of finite elements in electrical machines, phantom loading of machines as well as in the design and development of novel machines.

W. N. Fu was born in 1961 in Zhejiang, China. He received the B.Eng. and M.Eng. degrees in electrical engineering from Hefei University of Technology and Shanghai University of Technology, in 1982 and 1989, respectively. After graduation, he joined the Shanghai University as a Lecturer. Since 1994, he is a Visiting Scholar at the Hong Kong Polytechnic University. He has published over 45 papers in journals and international conferences. He completed a fully automatic mesh generation and mesh adaptation program by himself when he studied for M.Eng. degree. He independently developed a 2-D and 3-D circuit-field-torque coupled time stepping finite element package for simulation of induction motor, permanent magnet synchronous machine and brushless d.c. motor when he studied as Ph.D. student. His research interests include electromagnetic field computation, modem electric motor control and studies on novel machines. His research project currently is studying the performance of DSP controlled electric motors using control loop—FEM coupled method.